New Phytologist

Research

Key sources of uncertainty in process-based modeling of live fuel moisture content

Rodrigo Balaguer-Romano[1]*, Albert Sañé[1]*, Nicolas Martin-StPaul[2], Julien Ruffault[2], Eva Gabriel[3], Xavier Castro[4], François Pimont[2], Xiangzhuo Liu[2], Arsène Druel[2], Sylvain Delzon[5] and Miquel De Cáceres[1,6]

[1]CREAF, Bellaterra (Cerdanyola del Vallès), E08193, Catalonia, Spain; [2]INRAE-URFM, Domaine Saint Paul, 228 route de l'Aérodrome, Site Agroparc, CS 40509, 84914, Avignon Cedex 9, France; [3]Forest Ownership Centre, Government of Catalonia, Santa Perpètua de Mogoda, E08130, Barcelona, Spain; [4]Fire Prevention Service, Government of Catalonia, Santa Perpètua de Mogoda, E08130, Barcelona, Spain; [5]UMR BIOGECO, INRAE, Université de Bordeaux, Cestas, 33610, France; [6]CSIC, Bellaterra (Cerdanyola del Vallès), E08193, Catalonia, Spain

Author for correspondence:
Rodrigo Balaguer-Romano
Email: r.balaguer@creaf.uab.cat

Received: *10 March 2026*
Accepted: *6 May 2026*

New Phytologist (2026)
doi: 10.1111/nph.71286

Key words: drought stress, live fuel moisture content, MEDFATE, process-based modeling, SurEau-ECOS, wildfire danger.

Summary

- Process-based models that mechanistically represent water-carbon balances in the atmosphere-soil–plant continuum are an attractive tool for monitoring live fuel moisture content (LFMC) dynamics, a key variable when assessing fire danger. However, their application as operational tools to assess near-term wildfire danger at regional scale faces important challenges. Here, we explored key sources of prediction uncertainty in process-based modeling of LFMC.
- We applied the SurEau-ECOS model of plant hydraulics embedded within the MEDFATE modeling framework to assess how the accuracy of LFMC predictions was influenced by input data sources, by the availability of species-specific plant traits and by the level of mechanistic detail used to model water content of plant tissues.
- A lack of accurate data describing soil physical properties compromises the application of process-based models for predicting LFMC. Nonetheless, using global meteorological and vegetation data allows for successful regional-scale applications. Fully mechanistic approaches that model LFMC from plant water status using ecophysiological knowledge yield more accurate predictions. However, when reliable plant traits are lacking, semimechanistic approaches based on empirical equations offer a robust alternative.
- Overall, addressing the sources of uncertainty highlighted here could pave the way for developing operational tools to forecast near-term wildfire danger through process-based modeling of LFMC dynamics.

Introduction

The increasing incidence of extreme wildfire events is fueling efforts to improve our understanding of the climate–vegetation interactions underlying fire activity, as well as the monitoring of near-term fire danger (Nolan *et al.*, 2020; Rodrigues *et al.*, 2023). Fuel moisture content (FMC) expresses the ratio of water mass to dry mass contained in a vegetation component (i.e. live or dead stems, branches or foliage) and thus affects fire ignition probability, fire behavior and resultant fire severity (Pimont *et al.*, 2019; Boer *et al.*, 2021; McNeice *et al.*, 2026). Although live and dead FMC are both important determinants of fire activity, different mechanisms drive their respective spatial and temporal dynamics (Jolly *et al.*, 2014, 2025; Ruffault *et al.*, 2023). Dead FMC (DFMC) dynamics are often relatively fast and driven by daily weather conditions that affect the water content of fuels, while the dry mass is affected by slower decomposition processes only (Matthews, 2014). Thus, drought indices based solely on daily meteorological data are widely applied to monitor DFMC dynamics (Resco de Dios *et al.*, 2015). By contrast, the dynamics of live FMC (LFMC) are usually slower and are driven by fluctuations in both water and dry mass (Griebel *et al.*, 2023). These variations relate to processes that govern plant water and carbon balances and are regulated by species-specific plant anatomical and physiological traits (Jolly & Johnson, 2018). Thus, in addition to changes in weather conditions, live fuel water mass fluctuations relate to rooting patterns, plant hydraulic and stomatal regulation traits driving soil water uptake, plant water transport and the water content of plant organs (Nolan *et al.*, 2018). Meanwhile, dry mass fluctuations are governed by processes related to the plant carbon balance, including photosynthesis, respiration, tissue growth, senescence and phenology (Brown *et al.*, 2022). Therefore, it has been often argued that the incorporation of species-specific physiological and anatomical traits, together with the mechanistic understanding of water- and

*Theses authors contributed equally to this work.

carbon-related processes driving LFMC dynamics would enhance fire danger monitoring and forecasting capabilities (Jolly & Johnson, 2018).

Although meteorological drought indices are widely used to monitor DFMC, they fail to account for plant population structure, species-specific physiological adjustments, plant water-use strategies and phenology-driven fluctuations in dry mass, limiting their usefulness for LFMC monitoring (Ruffault *et al.*, 2018). Meanwhile, besides remote sensing approaches provide an opportunity to monitor LFMC dynamics over large spatial scales (Yebra *et al.*, 2018) at fine temporal resolutions (Quan *et al.*, 2024), they face inherent challenges in forecasting capability, which is crucial for effective wildfire risk assessment and management (Marino *et al.*, 2020). Also, field measurements are still needed to calibrate and validate physically based radiative transfer models or machine-learning algorithms that relate remotely sensed predictors with LFMC (Cunill-Camprubí *et al.*, 2022; Wang *et al.*, 2019). Under this backdrop, trait-enabled process-based models designed to mechanistically represent water, energy and carbon balances in forest ecosystems can address the limitations of meteorological drought indices and remote sensing approaches by allowing the explicit prediction of species-specific LFMC dynamics (Balaguer-Romano *et al.*, 2022; Ruffault *et al.*, 2023; Robbins *et al.*, 2025), as well as enabling forecasting capabilities (Balaguer-Romano *et al.*, 2023; Jia *et al.*, 2026). In process-based models, weather data are used as environmental forcing for water, energy and carbon balances (Sitch *et al.*, 2003; Ruffault *et al.*, 2022; De Cáceres *et al.*, 2023), while soil water balance is performed by estimating forest hydrological fluxes and considering soil physical properties related to soil water content and hydraulics. When plant hydraulics are modeled explicitly, water transport through the plant is simulated based on soil water availability and atmospheric demand, while considering physiological, phenological, anatomical and morphological traits regulating the water flow through vascular elements and thus the internal water content of the different plant tissues (Torres-Ruiz *et al.*, 2023). Process-based forest models that, in addition, consider carbon balance (i.e. photosynthesis, respiration), tissue growth, maturation and senescence processes can also be used to predict changes in fuel dry mass. Therefore, depending on their design, process-based models have the potential to simulate the fluctuations of both water and dry mass components of fuel moisture, making them an attractive tool for monitoring LFMC dynamics at different temporal and spatial resolutions (Torres-Ruiz *et al.*, 2023).

Notwithstanding the potential of process-based models, their application for monitoring and forecasting LFMC faces important challenges related to model complexity and input data requirements. There is a trade-off between how well the model design represents all relevant mechanisms and processes, and reducing the number of parameters needed to run the simulations, which affect model uncertainty and predictive ability (Dumedah & Walker, 2014). For example, LFMC could be modeled in a simplistic way by only considering the water content in the leaves, or it can be modeled more realistically by considering the water content for leaf and branch compartments independently and the seasonal changes in their relative proportions following defoliation processes (Ruffault *et al.*, 2023; Cakpo *et al.*, 2024), which in turn would lead to an increase in the parametrization and input data needed to run the simulations, thereby increasing results uncertainty. A way to partially overcome these plant trait-related uncertainties is to adopt semimechanistic approaches that reduce model complexity by using general empirical relationships between drought metrics (i.e. soil water content or predawn leaf water potentials, Ψ_{pd}) and LFMC values (Ruffault *et al.*, 2018; Balaguer-Romano *et al.*, 2022). While this strategy still requires a proper estimation of soil water balance, which is a key source of LFMC uncertainty, it nevertheless avoids the need of determining additional species-specific parameters relating water potential with the water content of live fuels. However, as semimechanistic LFMC predictions have been found to achieve moderate accuracy, potentially due to soil water balance uncertainties and the use of the same empirical relationships for species having different functional behavior (Balaguer-Romano *et al.*, 2022), exploring the potential of fully mechanistic approaches through the species-specific adjustment of the key anatomical and physiological emerges as a promising way to enhance LFMC monitoring capabilities (Nolan *et al.*, 2018; Ruffault *et al.*, 2023; Brown *et al.*, 2025). Nonetheless, it is important to note that even with the availability of plant trait databases such as TRY-Plant Trait Database (Kattge *et al.*, 2020) or the Xylem Functional Traits Database (XFT; Choat *et al.*, 2012), measurements of key traits related to plant hydraulics and water relations may be missing for a large number of target species, in particular when care is taken to filter and remove spurious data (Martin-StPaul *et al.*, 2017; Guillemot *et al.*, 2022).

The development of operational tools for assessing near-term wildfire danger using LFMC process-based modeling should also consider the availability of detailed and high-quality meteorological, soil and vegetation input data at regional scales. There is an expanding array of open-access products that can be used to address meteorological input data requirements, ranging from global reanalysis climate datasets, such as ERA5-Land (Muñoz-Sabater *et al.*, 2021), to interpolation tools that use local topography and meteorological data from weather stations (De Cáceres *et al.*, 2018; Thornton *et al.*, 2021). While site-specific vegetation composition and structure can be obtained from national forest inventories, other key functional variables such as leaf area index (LAI) can be estimated over large extents using remote sensing products (Myneni *et al.*, 2021) or allometric relationships derived from forest inventory data (Sánchez-Pinillos *et al.*, 2021). Finally, process-based models also incorporate specific modules to mechanistically represent soil water dynamics based on soil hydraulic properties data that implies a high degree of uncertainty due to inherent field measurement limitations (e.g. Loiseau *et al.*, 2023; Stocker *et al.*, 2023). Despite some soil physical characteristics can be obtained from global products at high resolution such as SoilGrids (Poggio *et al.*, 2021), rock fragment content (RFC) data that play a crucial role in affecting soil water content dynamics (Huang *et al.*, 2023) areusually missing, reducing the performance of soil water balance simulations and ultimately compromising the accuracy of LFMC predictions in process-based models.

In this study, we sought to explore the value of trait-enabled process-based modeling for operational LFMC prediction in a

Mediterranean context, by using a state-of-the-art modeling framework and evaluating the importance of key sources of prediction uncertainty. Specifically, we focused on how the accuracy of LFMC predictions was influenced by (1) the uncertainty in soil input data; (2) the source of meteorological and vegetation input data; and (3) the level of mechanistic detail used to model plant water status. Overall, we expected that accurate estimations of soil water availability would be key for reliable LFMC predictions, while the source of climate forcing and LAI would lead to lesser variation in prediction accuracy. In addition, we expected that higher level physiological and anatomical details involving the consideration of different tissue compartments and defoliation processes (i.e. model complexity) could lead to a better fit between LFMC predictions and observations when appropriate plant trait measurements for the target species are available.

Materials and Methods

LFMC sampling databases

We conducted the study using LFMC field data from two existing monitoring networks, the Catalan (NE Spain, Gabriel *et al.*, 2021) and the French Reseau–Hydrique (SE France, Martin-StPaul *et al.*, 2018). The combination of the two networks is relevant because they focus on similar tree and shrub species that are common in northwestern Mediterranean shrublands. Moreover, the two networks follow similar sampling protocols measuring the moisture content of live fine fuels, that is leaves and small branches foliar and stem (<6.35 mm). Specifically, sun-exposed apical and lateral green shoots of branches were collected *c.* 12:00 UT, placed in hermetic containers and transported to the laboratory, where they were weighed fresh (F_w). Then, after being oven dried at 100°C for 48 h and 60°C for 24 h respectively, samples were weighed dry (D_w) to finally estimate LFMC using (Eqn 1):

$$\mathrm{LFMC}(\%) = \frac{(F_w - D_w)}{D_w} \cdot 100 \qquad \text{Eqn 1}$$

We selected nine sampling sites from the Catalan network which covers the 2012–2019 period and 29 from Reseau–Hydrique, which covers the 2016–2019 period (Fig. 1), resulting in a subset of 38 sampling sites (Supporting Information Table S1). We selected LFMC observations sampled between the start of May to the end of September, as this period concentrates most of the drought episodes and therefore the highest fire danger (Resco De Dios, 2020). The final LFMC database comprised a total of 7203 LFMC values measured from 20 target species and 81 species-site combinations (summary of measured LFMC data by species and site available in Table S2).

Water balance simulations

To simulate soil and plant water balance in the 38 target sites, we employed MEDFATE, a process-based modeling framework designed to simulate forest functioning and dynamics specially

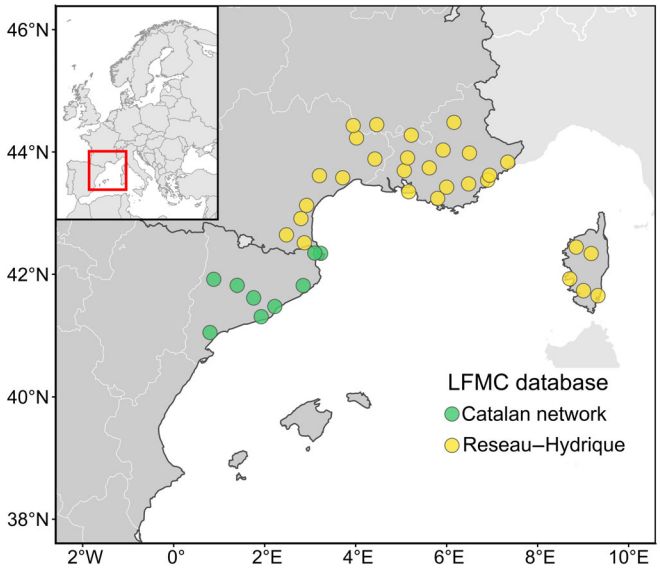

Fig. 1 Location of the selected live fuel moisture content (LFMC) sampling sites. Sites contained in the Catalan network (Gabriel *et al.*, 2021) in green and the French Reseau–Hydrique network (Martin-StPaul *et al.*, 2018) in yellow.

designed for Mediterranean areas (De Cáceres *et al.*, 2023). The framework provides different submodels and is accessible through R packages MEDFATE (v. 4.8.4) and MEDFATELAND (v. 2.7.1). The framework allows performing soil and plant water balances in forest stands given appropriate soil, vegetation and daily weather inputs. Vegetation is represented using a set of woody plant cohorts representing individuals of the same size and species identity. Soils can be vertically stratified into layers of different depths, each with different textural and structural properties. Plant cohorts can have different vertical distribution of roots among soil layers but, since the model is essentially one dimensional (i.e. not spatially explicit), by default, there is no horizontal separation between root systems. However, in this study, we performed water balance simulations assuming that the rhizosphere of each plant cohort draws water primarily from its own water pool but allowing to dynamically adapt the degree of rhizosphere overlap between cohorts depending on the hydraulic conductivity of the soil. This option has the advantage of accounting for interspecific interaction for water resources at the beginning of dry periods (i.e. soil moisture is depleted slower or faster depending on species composition), while allowing different plant water potentials during periods of severe edaphic drought, when soil hydraulic conductivity is low and the rhizospheres of different plants are isolated from each other (Moreno *et al.*, 2024).

MEDFATE can perform soil and plant water balances using different levels of mechanistic detail depending on submodel choices. In this work, we employed a dual-porosity submodel (Larsbo *et al.*, 2005) to simulate water fluxes within the bulk soil, which allows separating preferential flows through macropores from unsaturated flows in the soil matrix. Importantly, we used the implementation of the SurEau-ECOS model

(v.2.0) (Ruffault *et al.*, 2022) within MEDFATE as a submodel for the computation of plant hydraulics and transpiration processes. SurEau-ECOS offers a detailed trait-based plant hydraulics modeling framework that provides an improved representation of the dynamics of water storage and water transport within plants. It includes a representation of the apo- and symplastic compartments in two primary organs (leaves and stems) and allows considering water losses through stomata and the cuticle, providing a comprehensive understanding of plant water transport and desiccation under extreme drought stress. In MEDFATE, the plant hydraulics provided by SurEau-ECOS are coupled with additional processes that are simulated at subdaily time steps, namely the canopy and soil energy balance, leaf energy balance, plant photosynthesis and stomatal regulation (De Cáceres *et al.*, 2021). Water balance simulations produce daily and subdaily predictions of water potential (Ψ) along different nodes (fine roots, root crown, stem and leaves) of the soil–plant–atmosphere continuum, as well as the proportion of conductance loss (PLC) in xylem tissue of leaves and stems. PLC increases during dry periods, and MEDFATE uses PLC to reduce LAI because of drought-induced defoliation. Since simulations of this study encompassed several years but growth was not represented, we assumed a complete recovery of conductance and LAI between 1 yr and the next. MEDFATE-SurEau implementation has been proven to provide robust estimations of water and carbon balances within forest ecosystems (Saponaro *et al.*, 2025).

LFMC modeling approaches

We explored one 'semi-mechanistic' and three 'fully mechanistic' approaches to model LFMC from plant water status (i.e. leaf water potential). We use the term 'semi-mechanistic' when plant water status is simulated with the process-based model, but LFMC is estimated through an empirical relationship (Balaguer-Romano *et al.*, 2022), and the term 'fully mechanistic' when both plant water status and LFMC are modeled using ecophysiological knowledge (e.g. Ruffault *et al.*, 2023; Jolly *et al.*, 2025). Both approaches ignore variations in water content related to ontogenetic changes during leaf maturation, so LFMC modeling focuses on mature leaves. This is because the weak links between tissue water content changes and water potential during the immature stage of leaves result in high LFMC ranges that have negligible effects on fire danger (Pimont *et al.*, 2019). However, this could be a limitation as the leaf-out phenology of some Mediterranean forest species, such as *Quercus coccifera* L., drive changes in LFMC values (Fares *et al.*, 2017).

Semimechanistic modeling LFMC approach The semimechanistic approach ($LFMC_{semi}$) of Balaguer-Romano *et al.* (2022) is based on the fact that LFMC variation has been shown to be effectively predicted from variation in predawn leaf water potentials (Ψ_{pd} MPa; Nolan *et al.*, 2018). This modeling approach employs MEDFATE to predict Ψ_{pd}, which serves as the mechanistic component, and then combines this output with an empirical logarithmic relationship between Ψ_{pd} and LFMC (Eqn 2):

$$LFMC_{semi} = 91.87 - \left(31.12 \cdot \log\left(-\Psi_{pd}\right)\right) \quad \text{Eqn 2}$$

This empirical relationship has been previously calibrated and validated using simulated Ψ_{pd} values and field-measured LFMC data from Mediterranean tree and shrub species, making it suitable to be applied in this study. Also, the accuracy of LFMC predictions simulated with the semimechanistic approach has been previously compared with predictions derived from widely used approaches such as drought indices or remote sensing (Balaguer-Romano *et al.*, 2022). Therefore, we considered the results of the semimechanistic simulation as benchmarks against which to compare the performance of fully mechanic approaches.

Fully mechanistic modeling LFMC approaches In the remaining set of approaches, LFMC was dynamically modeled from leaf and upper stem water potentials estimated in apo- and symplastic compartments, using pressure–volume relationships between water potential (Ψ; MPa) and relative water content (RWC; %). Specifically, (1) the model first estimates RWC in leaf or stem symplastic tissues from the water potential in those compartments using pressure–volume curves (Bartlett *et al.*, 2012), and (2) it takes the one complement of the PLC lost in leaves and stem (i.e. $1 - PLC_{leaf}$ and $1 - PLC_{stem}$) as the surrogate of RWC in the apoplastic (xylem) compartment of leaves or stem, respectively (Ruffault *et al.*, 2023). The fraction of apoplastic tissue in each organ is then employed to weigh the RWC of sym- and apoplastic compartments, which leads to the estimation of RWC for leaves and stems, that is RWC_{leaf} and RWC_{stem}, respectively. Finally, subdaily temporal variation of RWC_{leaf} and RWC_{stem} (resulting from subdaily variation in water potentials) are averaged before LFMC estimation.

We tested three different 'fully mechanistic' approaches to estimate LFMC. In the first one, $LFMC_{full1}$, we assumed that temporal variation in LFMC could be simply modeled as the product of the species-specific LFMC at full hydration (FMC_{max}) and the modeled leaf RWC (Eqn 3).

$$LFMC_{full1} = FMC_{max} \cdot RWC_{leaf} \quad \text{Eqn 3}$$

In the second and third approaches ($LFMC_{full2}$ and $LFMC_{full3}$), we acknowledged that live fine fuels are in fact composed of stems (<6.35 mm) and the attached leaves. Therefore, LFMC values were estimated considering both RWC, RWC_{leaf} and RWC_{stem} (Eqn 4):

$$LFMC = FMC_{leafmax} \cdot f_{leaf} \cdot RWC_{leaf} + FMC_{stemmax} \cdot \left(1 - f_{leaf}\right) \cdot RWC_{stem} \quad \text{Eqn 4}$$

where f_{leaf} is the ratio of foliar (photosynthetic) biomass to foliar and stems (<6.35 mm) biomass, and $FMC_{leafmax}$ and $FMC_{stemmax}$ are the maximum moisture content (%) of leaves

and branches, respectively. They are related to the maximum LFMC value (FMC_{max}) as follows (Eqn 5):

$$FMC_{max} = FMC_{leafmax} \cdot f_{leaf} + FMC_{stemmax} \cdot (1 - f_{leaf}) \quad \text{Eqn 5}$$

Note S1 details how species-specific $FMC_{leafmax}$ and $FMC_{stemmax}$ can be estimated from wood density, f_{leaf} and FMC_{max} given as species-specific parameter inputs (see also Jolly *et al.*, 2025, for an alternative way to estimating LFMC in leaves). The difference between $LFMC_{full2}$ and $LFMC_{full3}$ relies on the consideration of seasonal dynamics in f_{leaf}. Therefore, while in $LFMC_{full2}$, we assumed f_{leaf} as constant (i.e. $f_{leaf} = f_{leafmax}$), in $LFMC_{full3}$, we took the assumption that defoliation in sampled stems followed plant defoliation as acknowledged in Ruffault *et al.* (2023) and Cakpo *et al.* (2024), which in MEDFATE was estimated using PLC_{leaf} (Eqn 6; Cakpo *et al.*, 2024):

$$f_{leaf} = f_{leafmax} \cdot (1 - PLC_{leaf}) \quad \text{Eqn 6}$$

where $f_{leafmax}$ is a species-specific parameter indicating the (maximum) ratio of foliar (photosynthetic) biomass to foliar and stem (<6.35 mm) biomass. Note that even though we call these three approaches 'fully mechanistic', they involve an increasing degree of mechanistic detail from $LFMC_{full1}$ to $LFMC_{full3}$.

Input data sources and simulation design

Soil input properties Soil physical properties across different depths, such as texture (i.e. volume percent of sand, silt and clay), organic matter content and bulk density, influence MEDFATE water balance modeling by defining the soil moisture retention and hydraulic conductivity curves. These, together with RFC, define the soil total available water (TAW) for a given depth. We discretized the soil of each target site into five layers with the following depths: 0–150 mm, 150–300, 300–600, 600–1000 and 1000–2000 mm. We obtained for each layer clay and sand percentage, bulk density, organic matter content and RFC values at a spatial resolution of 250 m from SoilGrids 2.0 database (Poggio *et al.*, 2021). As SoilGrids tends to underestimate RFC (RFC, %), we initially adjusted RFC using global maps with specific data of soil depth and bedrock probability (Shangguan *et al.*, 2017). Then, we took the soil texture and structure estimates as constant but tested a range of TAW values as input values for simulations (expanded in section Simulation design).

Meteorological input alternatives Daily weather data (including minimum and maximum atmospheric temperature, minimum and maximum relative humidity, total precipitation, solar radiation and wind speed) are the environmental forcing of MEDFATE water balance modeling. We compared the accuracy of LFMC predictions between two alternative sources of weather data appropriate for simulation over large extents: (1) ERA5-Land reanalysis data (Muñoz-Sabater *et al.*, 2021) vs (2) distance-based weather interpolation from weather station data using METEOLAND R package (De Cáceres *et al.*, 2018). For the latter case, weather station data were obtained from the Catalan Meteorological Service, the Spanish Meteorological Agency and the French Meteorological Agency. Both sources were selected aiming at the comparison between globally available and locally derived products of daily weather data. Thus, while ERA5-Land reanalysis data are provided at a pixel resolution of 9 km, the (nominal) resolution of the interpolated data is defined by the topographic map, being 30 m in this study.

Vegetation data and leaf area index estimation alternatives We used vegetation structure and species composition data from field surveys conducted on each of the 38 sampling sites as input for water balance simulations. Vegetation data included the mean height and percent cover of all woody species present, including those beyond the target species for LFMC monitoring. Stand-level LAI, representing the total one-sided area of leaf tissue per unit ground surface area, is a key variable for MEDFATE process-based water balance modeling as it strongly modulates evaporation and transpiration fluxes and, hence, plant drought stress. As for meteorological input, we aimed the comparison between globally available and locally derived data. Thus, we compared the accuracy of LFMC predictions between two alternative methods of determination of stand-level LAI: (1) the MODIS product MCD15A2H v.6 (Myneni *et al.*, 2021) vs (2) the sum of species-level LAI estimates obtained from vegetation data via allometric relationships (Sánchez-Pinillos *et al.*, 2021). The MODIS product provides LAI data (hereafter MODIS-LAI) with a spatial resolution of 500 m and a temporal resolution of 8 d. We estimated a unique MODIS-LAI value per sampling site by averaging 2002–2024 yearly values. To minimize the potential errors derived from vegetation phenology, we first processed annual values by averaging the five highest LAI values of each year, assuming these values would correspond to the periods of fully developed foliage in deciduous species (Balaguer-Romano *et al.*, 2025). On the other hand, species-level LAI estimates were obtained by applying existing allometric relationships (Sánchez-Pinillos *et al.*, 2021) between plant cover/height values and fine fuel biomass, followed by the multiplication by the fraction of leaves, f_{leaf}, and specific leaf area (SLA). Finally, the stand-level allometry-based LAI estimate was then obtained by summing the LAI values of all species occurring within each sampling site.

Species-specific plant traits Species-specific trait parameter values (Table S3) were obtained using three approaches: (1) species-level statistics obtained from published plant-trait data sources (De Cáceres *et al.*, 2023); (2) trait measurements performed by URFM (Mediterranean Forest Research Unit of INRAE, Avignon) on the Reseaux Hydrique sites; (3) trait-specific imputation rules. Many model parameters were matched to plant traits drawn from the TRY public dataset (v.5.0; https://www.try-db.org/, last access: 30 May 2023; Kattge *et al.*, 2020), complemented by additional databases, global analysis papers and personal compilations for phenology, anatomy and morphology (Morris *et al.*, 2016; Tavşanoğlu & Pausas, 2018), plant hydraulics (Choat *et al.*, 2012; Martin-StPaul *et al.*, 2017; Mencuccini *et al.*, 2019; Sanchez-Martinez *et al.*, 2020), pressure–volume curves (Bartlett *et al.*, 2022) and

stomatal or cuticular conductance (Hoshika *et al.*, 2018; Duursma *et al.*, 2019; Burlett *et al.*, 2025). In particular, values of LFMC at full hydration (FMC_{max}) were obtained using 95% quantiles on values reported in Yebra *et al.* (2024). Whenever possible, we replaced bibliographic values by physiological measurements (pressure–volume curves, xylem hydraulic conductivity vulnerability curves, water potential at turgor loss point and cuticular conductance) performed by URFM.

Missing values for physiological and anatomical parameters were imputed using species-specific rules. Rooting depth, classified as the depth at which cumulative 95% (Z95) of fine roots occur, was imputed for all species following Balaguer-Romano *et al.* (2022) according to plant functional groups. Thus, seeder shrub species were imputed with a Z95 value of 400 mm, resprouting shrubs with 1500 mm and tree species with 2500 mm. Then, the depth at which cumulative 50% and 100% (Z50 and Z100) of fine roots occur was estimated using logarithmic relationships with Z95. When not available from measurements, values for f_{leaf} and SLA were obtained from average values for combinations of leaf shape and leaf size. Also, missing values for photosynthetic parameters (V_{cmax} and J_{max} at 25°C) were estimated from SLA and N_{leaf} values (Walker *et al.*, 2014). Missing values for pressure–volume curves and apoplastic fraction of leaf tissue were estimated using family-level means, while pressure–volume curves of stem symplastic tissue were estimated from wood density following Christoffersen *et al.* (2016). Finally, missing values for stomatal or cuticular conductance and xylem vulnerability curves were obtained using family-level means, and water potential values corresponding to 50% stomatal closure were imputed from the water potential at the turgor loss point.

Simulation design First, we tested the effect of calibrating soil properties over the accuracy of LFMC predictions by inputting a range of soil TAW values. Specifically, we linearly varied the RFC of soil layers, previously modified following Shangguan *et al.* (2017) so that a range of TAW values were tested between 30 and 200 mm using 10-mm steps. Then, we explored how different input data sources of daily meteorological values and LAI influence the fit between observed and predicted LFMC dynamics simulated at each species-site combination. Also, all simulations were run for the four LFMC modeling approaches, that is the semimechanistic ($LFMC_{semi}$) and the three fully mechanistic approaches ($LFMC_{full1–3}$). Therefore, we simulated LFMC dynamics across 81 species-site combinations that were run under a range of 18 different soil TAW, under two different meteorological and two LAI input data sources and applying four modeling approaches, resulting in a total of 23 328 unique simulations of LFMC dynamics.

Data analyses

Model performance evaluation Since field samples were measured from May to September, some observed LFMC values could correspond to immature leaves for some species depending on their leaf-out phenology. Also, LFMC values simulated by applying the fully mechanistic modeling approaches were bound to species-specific FMC_{max} values. Therefore, we considered LFMC observations higher than FMC_{max} as outliers to focus the modeling on mature leaves. This led to discarding 249 observations (3.5%), resulting in a final subset of 6954 LFMC observations used for model evaluation. We established the accuracy of each simulation by performing linear regressions between observed and predicted LFMC and calculating the mean absolute error (MAE) and the coefficient of determination (R^2).

Assessment of the effect of simulation factors We assessed the effect of simulation factors (i.e. soil TAW, LAI, meteorological input data and modeling approaches) over the accuracy of LFMC predictions, reducing the degree of interaction among factors by gradually fixing the values that resulted in the best fit. Thus, we first explored the effects of soil TAW variation over the accuracy of LFMC predictions across the whole simulation set ($n = 23\,328$ simulations). Then, we assessed how the meteorological and LAI input data sources affected the accuracy of LFMC predictions by analyzing the simulations run with the TAW value that resulted in the best fit ($n = 1296$ simulations). Next, we explored how the source of hydraulic trait data (i.e. bibliographic/measured vs imputation) affected the accuracy of LFMC predictions in each modeling approach by assessing the simulations run with the TAW value and with the meteorological and LAI data sources that resulted in the best fit ($n = 324$ simulations). Finally, we compared how the different modeling approaches performed LFMC predictions by assessing the simulations that resulted in the best fit at each species-site combination ($n = 81$ simulations). We employed the paired *t*-test to assess significant differences ($P < 0.05$) among meteorological and LAI values obtained from different data sources, and among the accuracy of LFMC predictions of each modeling approach when run with different hydraulic trait data sources.

Results

Soil calibration effects on LFMC prediction

The accuracy of LFMC predictions varied depending on the soil TAW value used to run the simulations. Thus, the whole set of simulations run with different TAW values ($n = 23\,328$ simulations) resulted in R^2 metrics that ranged from 0 to 0.84 with an average of $0.25 \pm 0.8 \times 10^{-5}$ (Fig. 2a), and MAE metrics that ranged from 5.1 to 111.4% with an average of $24.1\% \pm 0.6 \times 10^{-3}$ (Fig. S1). The best accuracy in LFMC predictions was obtained from simulations run with 110 mm as TAW, with an average R^2 of $0.27 \pm 0.1 \times 10^{-3}$ and MAE of $24\% \pm 0.01$. Conversely, simulations run with a TAW value of 30 mm resulted in the poorest fit metrics, with an average R^2 of $0.17 \pm 0.1 \times 10^{-3}$ and MAE of $22\% \pm 0.01$. Overall, the accuracy of LFMC predictions was better when the TAW was close to 100 mm, while the fit decreased at both extremes of TAW range, that is 30 and 200 mm (Fig. 2a). This was consistent with the final set of simulations that achieved the best fit for each species-site combination ($n = 81$ simulations), as a higher number of best fit species-site simulations were run with 90 and 110 mm as

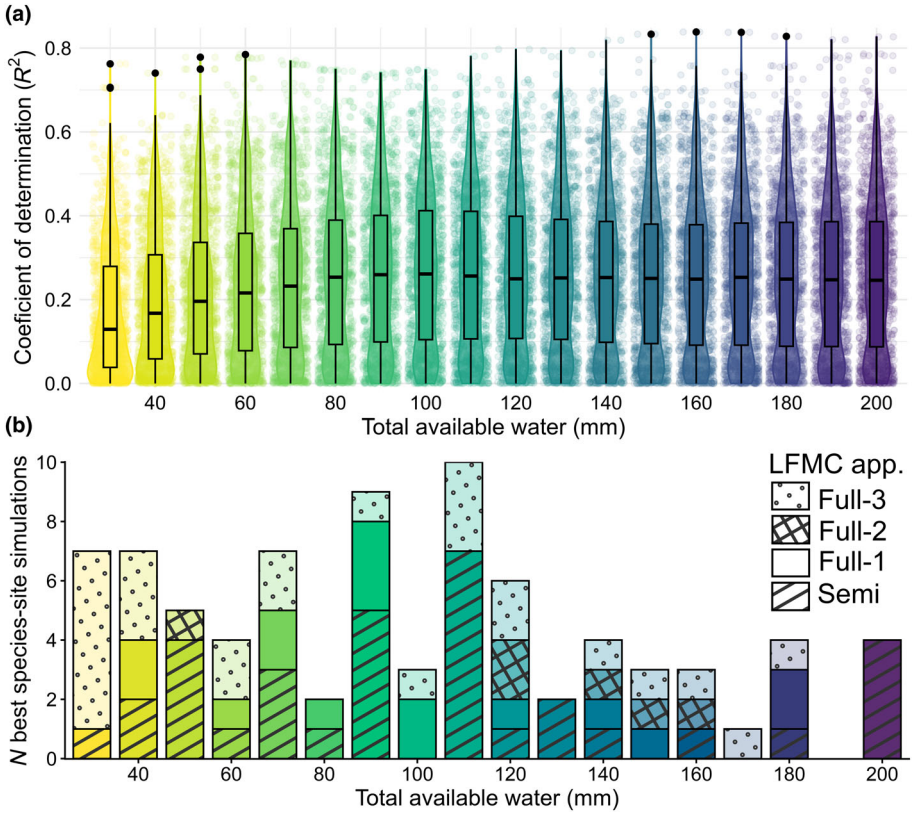

Fig. 2 Soil total available water (total available water (TAW) mm, color gradient) effect over the accuracy of live fuel moisture content (LFMC) predictions. (a) Distribution of the coefficient of determination (R^2) resulting from the fit between observed and predicted LFMC simulated for a set of TAW values ranging from 30- to 200-mm at 10-mm steps. In box plots, the horizontal line indicates the median, the box represents the interquartile range (IQR), and the whiskers extend to the most extreme data points within 1.5 times the IQR. Individual dots represent outliers. (b) Distribution of the TAW values that resulted in the best fit between observed and predicted LFMC in each species-site combination (size (N) = 81 simulations). Bars shade type refers to the LFMC modeling approach applied in each species-site simulation, that is, the semi-mechanistic ($LFMC_{semi}$) and the three fully mechanistic approaches ($LFMC_{full1-3}$).

soil TAW values (Fig. 2b). Nonetheless, at some species-site combinations, the highest accuracy in LFMC predictions was obtained under soil TAW values *c.* 30–40 mm. These species-site combinations mostly correspond with seeder shrub species such as *Cistus* spp. and *Salvia rosmarinus* Spen., while species-site combinations that showed the best fit under soil TAW values *c.* 180–200 mm mostly correspond to tree species such as *Quercus ilex* L. and *Pinus halepensis* Mill. (Table S4).

Meteorological and LAI input data effects on LFMC prediction

We found differences in climate inputs and LAI values between data sources at each study site (Table S1). We estimated the mean annual precipitation (MAP) and the mean annual temperature (MAT) from both data sources (ERA5-Land and weather interpolation) at each study site using the meteorological series of the whole simulation period. MAP values obtained from ERA5-Land ($\overline{x} = 823$ mm $\pm$ 5 mm) and from weather interpolation (805 mm $\pm$ 4 mm) were not significantly different ($P = 0.47$ in a paired test), but moderately correlated ($r = 0.58$, $P < 0.001$). However, MAT obtained from ERA5-Land (14°C $\pm$ 0.05°C) was significantly lower ($P < 0.001$ in a paired test) than the MAT obtained using weather interpolation (15.4°C $\pm$ 0.04°C). Despite this difference, the two MAT estimates were strongly correlated ($r = 0.88$, $P < 0.001$). Meanwhile, MODIS-LAI values ($\overline{x} = 2.38 \pm 0.01$) were significantly higher ($P < 0.001$) than LAI values estimated through allometric equations ($\overline{x} = 1.59 \pm 0.02$), and both values were not significantly correlated ($r = 0.1$, $P = 0.56$).

The accuracy of LFMC predictions showed different degrees of fit depending on the meteorological and LAI data source combination (Fig. 3) when analyzing the simulations run with the TAW value that resulted in the best fit at each species-site combination ($n = 1296$ simulations). The highest accuracy in LFMC predictions was always obtained in simulations run with meteorological data derived from ERA5-Land, independently of the LAI data source. Accordingly, using daily weather data from ERA5-Land instead of weather interpolations resulted in higher fit metrics for the semimechanistic modeling approach ($\Delta R^2 = 0.05$; $\Delta MAE = 2\%$) and even greater improvements for the three fully mechanistic approaches ($\Delta R^2 = 0.1$; $\Delta MAE = 4\%$). The two LAI data sources led to different levels of agreement between observed and predicted LFMC, although their effects were weaker than those caused by differences in meteorological data sources. Simulations run with MODIS-LAI data resulted in LFMC predictions with slightly higher accuracy than simulations run with LAI values estimated through allometric equations ($\Delta R^2 = 0.01$ and $\Delta MAE = 1\%$).

Modeling approach effects on LFMC prediction

The source of hydraulic trait values (bibliographic/measurements vs imputation) did not significantly affect the accuracy of LFMC predictions when simulated applying $LFMC_{semi}$, $LFMC_{full1}$ and $LFMC_{full2}$ modeling approaches. However, prediction accuracy

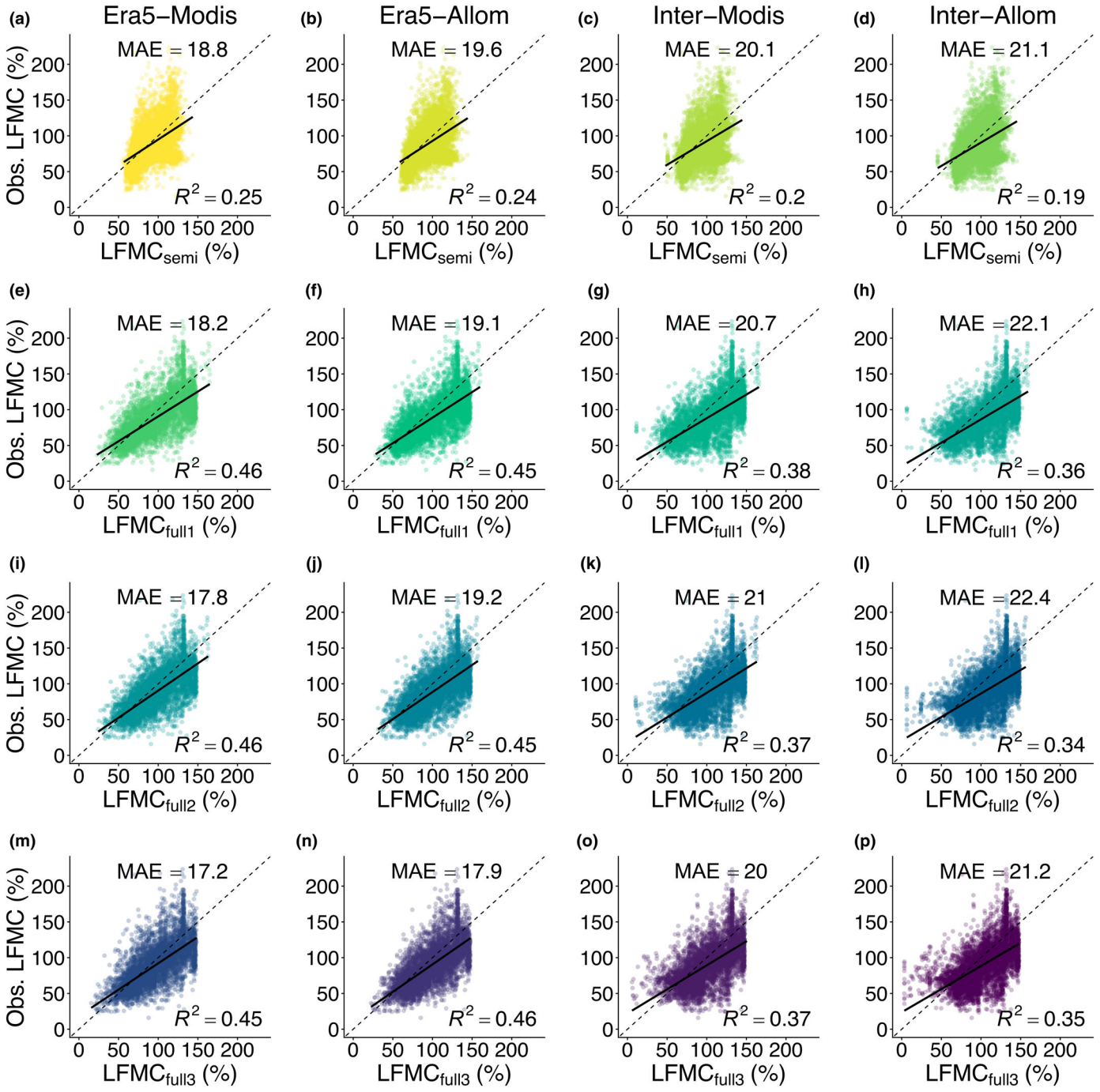

Fig. 3 Observed live fuel moisture content (LFMC) (%) against predicted values simulated under the semimechanistic approach (LFMC$_{semi}$: plots a–d), and the three fully mechanistic approaches (LFMC$_{full1}$: plots e–h, LFMC$_{full2}$: plots i–l and LFMC$_{full3}$: plots m–p). Simulations were run with the total available water value that resulted in the best fit and with combinations of meteorological and leaf area index (LAI) input data obtained from different sources. Meteorological data were obtained from ERA5-Land reanalysis (Era5) or from weather interpolation (Inter), while LAI data were obtained from a MODIS remote sensing product (Modis) or estimated through allometric equations (Allom). Plots mean absolute error (%), coefficient of determination (R^2) and red lines indicate the fit between observed and predicted LFMC. Color gradient indicates each modeling approach and input data combination.

was significantly higher when inputting plant traits derived from data sources in simulations run with the fully mechanistic approach LFMC$_{full1–3}$ (Figs 4, S2). Overall, fully mechanistic simulations achieved higher accuracy in LFMC predictions compared with semimechanistic ones under all meteorological and LAI input data source combinations (Fig. 3). More specifically, fully mechanistic modeling approaches (LFMC$_{full1–3}$) achieved the highest accuracy in LFMC predictions in 47 of 81 species-site combinations (Fig. 1b; Table S4). This is in line with the potential capabilities of fully mechanistic approaches to predict LFMC

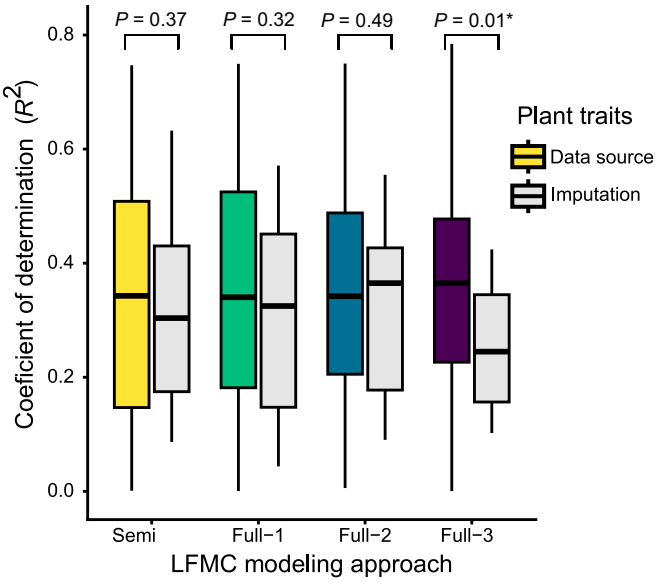

Fig. 4 Distribution of the coefficient of determination (R^2) resulting from the fit between observed and predicted live fuel moisture content in each species-site combination simulated under the four modeling approaches (semimechanistic in yellow, fully mechanistic 1–3 in green, blue and purple) according to if hydraulic plant trait values were derived from bibliographic/measurement data-sources (colored) vs imputation (gray). The *P*-values indicate the paired *t*-test significant level of the differences between R^2 metrics obtained using plant-traits from data-sources or imputation for each modeling approach. In box plots, the horizontal line indicates the median, the box represents the interquartile range (IQR), and the whiskers extend to the most extreme data points within 1.5 times the IQR.

values in the upper and lower range, as both plant water status and LFMC are modeled using detailed ecophysiological knowledge. Thus, as exemplified in Fig. 5a, fully mechanistic approaches allowed the prediction of the *Salvia rosmarinus* intra-annual LFMC seasonal variations, from the maximum values *c.* 120–140% at the beginning of the spring to the minimum values of 60–50% reached at the end of the summer, and the latter increase in LFMC values following autumn rains. By contrast, in the semimechanistic approach, the LFMC prediction range was limited by the empirical relationship applied to estimate LFMC from predawn leaf water potential values. This resulted in an inability to predict either the maximum LFMC values during spring, which remained below 120%, or the minimum values during summer, which in any simulated year fell below 70% (Fig. 5a).

Nonetheless, the semimechanistic modeling approach ($LFMC_{semi}$) was the most accurate in LFMC predictions in 34 species-site combinations. This better performance of the semimechanistic approach was related to either an inappropriate parameterization of the fully mechanistic approaches or their inability to simulate phenological carbon fluctuations that drive LFMC dynamics with greater intensity in certain species. In these cases, the empirical relationship applied to estimate LFMC from predawn leaf water potential in the semimechanistic approach avoided fully mechanistic modeling limitations and provided a more accurate and robust assessment of LFMC. Thus, as exemplified in Fig. 5b, the predictions obtained through fully mechanistic approaches remained at the *Arbutus unedo* L. maximum LFMC values 140% with almost no intra-annual variations. Meanwhile, semimechanistic predictions allowed the simulation of LFMC summer declines to values *c.* 80%, but temporarily ahead of the observed values, at least during the last years of the simulation (Fig. 5b).

Discussion

This study evaluates how key sources of prediction uncertainty affect the performance of process-based modeling of LFMC dynamics. As expected, an accurate estimation of soil water availability was a key input variable driving the accuracy of LFMC predictions. Meanwhile, the source of daily weather and stand-level LAI input data led to lesser variation in prediction accuracy, with global products resulting in more accurate LFMC values than local data sources. The level of mechanistic detail used to model plant water status also played a key role driving the accuracy of LFMC predictions. Fully mechanistic modeling approaches resulted in more accurate predictions when reliable plant traits data were available. Nonetheless, the use of semimechanistic approaches based on empirical equations resulted in a more robust strategy when reliable input data were missing.

The lack of accurate input data describing the physical properties that drive soil hydraulics resulted as the main source of uncertainty when simulating water balances across the atmosphere-soil–plant continuum. The calibration of RFC carried out by testing a range of soil TAW values largely affected the accuracy of LFMC predictions (Fig. 2a). The highest simulation accuracy at each species-site combination was obtained for different TAW values (Fig. 2b; Table S4). This highlights that LFMC dynamics are driven by both the species-specific traits that regulate water uptake from soil reservoirs and the site-specific environmental conditions and physical properties that define soil hydraulics at different depths (Dukes *et al.*, 2026). Nonetheless, global products and datasets fail in providing reliable estimates of RFC and soil depth to bedrock, which are crucial physical properties driving soil water dynamics (Huang *et al.*, 2023). This ultimately hinders the applicability of process-based models to predict LFMC within operational contexts, as site-specific estimations of optimum soil TAW values through the calibration of RFC input data at different soil depths is a time-consuming approach. A potential solution for the lack of reliable data on soil depth and RFC under forest areas could rely on inferring soil TAW through inverse modeling. That is, it could be assumed that a trade-off between plant water use and drought stress drives vegetation toward an ecohydrological equilibrium (Cabon *et al.*, 2018), which would imply that vegetation optimizes LAI to maximize transpiration within the seasonal limits of soil TAW values. This would give room to use dynamic series of LAI values derived from remote sensing products for inferring through inverse modeling procedures soil TAW temporal dynamics at large spatial scales (Stocker *et al.*, 2023), which could be finally used as input data for predicting LFMC through process-based modeling

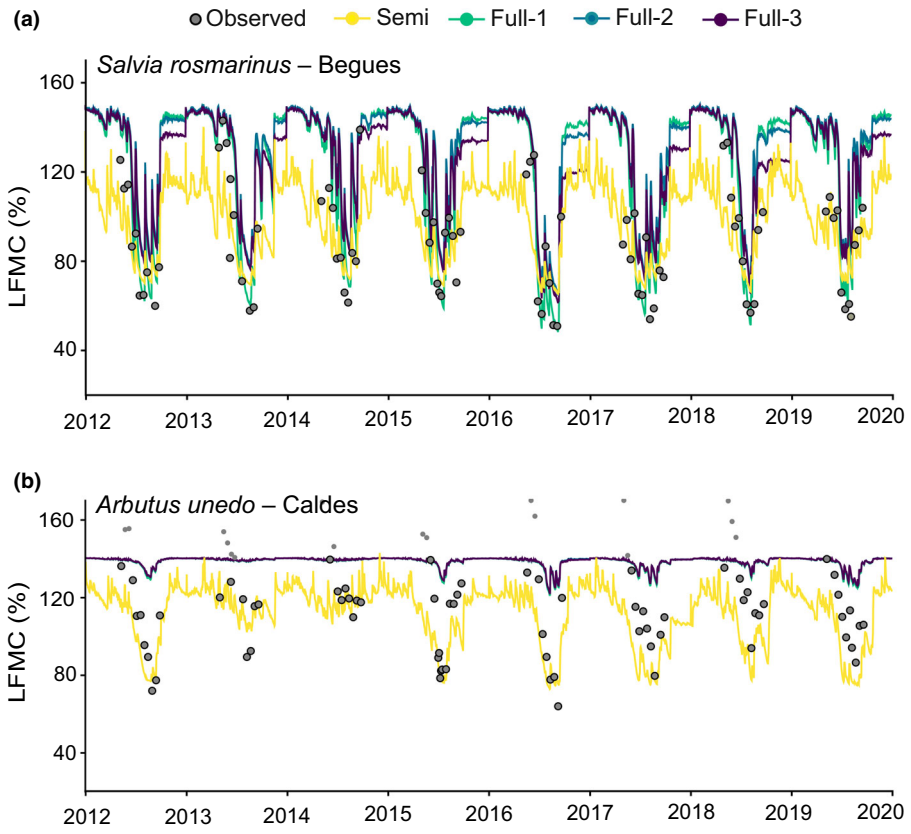

Fig. 5 Live fuel moisture content (LFMC) (%) dynamics from 2012 to 2020. Observed values are represented with gray filled black dots (outliers only in gray) while simulated time series under each modeling approach are represented in colored lines ($LFMC_{semi}$ in yellow, $LFMC_{full1}$ in green, $LFMC_{full2}$ in blue and $LFMC_{full3}$ in purple). Plot (a) corresponds to the species-site combination *Salvia rosmarinus*-Begues with 85 observed LFMC values. Optimum simulations were run with a TAW of 90 mm, meteorological data interpolated and LAI data derived from allometries. Each modeling approach simulation accuracy was $R^2 = 0.62$, MAE = 12.6% for $LFMC_{semi}$; $R^2 = 0.65$, MAE = 20.3% for $LFMC_{full1}$; $R^2 = 0.66$, MAE = 27.7% for $LFMC_{full2}$; $R^2 = 0.68$, MAE = 24.9% for $LFMC_{full3}$. Values in plot (b) corresponds to the species-site combination *Arbutus unedo*-Caldes de Malavella with 71 observed LFMC values. Optimum simulations were run with a total available water of 200 mm, meteorological data interpolated and leaf area index data derived from allometries. Each modeling approach simulation accuracy was $R^2 = 0.57$, MAE = 14.5% for $LFMC_{semi}$; $R^2 = 0.59$, MAE = 26.8% for $LFMC_{full1}$; $R^2 = 0.59$, MAE = 27.2% for $LFMC_{full2}$; $R^2 = 0.59$, MAE = 27.2 for $LFMC_{full3}$. All species-site combination plots are available in Supporting Information Fig. S3. MAE, mean absolute error.

approaches. Overcoming the lack of reliable data on the soil physical properties determining soil water capacity should be at the forefront of future research efforts aiming at the modeling of LFMC dynamics.

The application of process-based LFMC modeling in operational near-term wildfire danger assessments would require input data available at large spatial scales. In this regard, we compared the accuracy of LFMC predictions from simulations run using meteorological and LAI input data obtained from globally available and locally derived products (Fig. 3). The improved performance obtained using the ERA5-Land product may be related to the data gaps observed in meteorological daily time series at some weather stations used in weather interpolation. Thus, despite the higher spatial resolution of weather interpolation, the dependence on weather stations data availability and quality conditioned simulation performance. Also, the lower accuracy in predictions obtained using interpolated weather data could be due to the high uncertainty associated with the interpolation of precipitation events at a daily scale. In this regard, ERA5-Land data showed a better physical consistency between weather variables despite its coarser spatial resolution. In line with this, one potential improvement would be to downscale ERA5-Land climate data to finer spatial resolutions using, for example, kriging approaches informed by topography (Davy & Kusch, 2021) or direct downscaling methods driven by topographic (Druel *et al.*, 2025). MODIS-LAI data source also resulted in more accurate LFMC predictions despite the higher spatial resolution (500 m) compared with site- and species-specific allometric equations. Moreover, both LAI data sources were significantly different and not correlated. This could indicate that sample sizes used to develop species-specific allometric equations (Sánchez-Pinillos *et al.*, 2021) were not sufficiently representative and thus fail in providing reliable estimates when applied at large scales. Also, further errors may arise from the need to impute allometric equations from other species in those species with missing equations. Broadly, the higher simulation accuracy resulted from input data

derived from global products (ERA5-Land and MODIS-LAI) supports the applicability of process-based LFMC modeling at large scales, while avoiding the time needed to develop and/or calibrate local-derived products such as weather interpolation or plant allometric equations.

Beyond the soil physical properties and the meteorological conditions, LFMC temporal and spatial dynamics are driven by the plant ecophysiological processes that govern water and carbon cycles regulated by species-specific traits (Jolly & Johnson, 2018). For example, shrub species such as *Cistus* spp. and *S. rosmarinus* usually show poorer stomatal controls (Resco De Dios, 2020) and develop shallower root systems, which cannot reach deeper soil water sources (Nolan *et al.*, 2018: Ruffault *et al.*, 2018), leading to the largest seasonal LFMC variations. By contrast, tree species such as *Pinus halepensis* and *Quercus ilex* develop deeper root systems and show stronger stomatal controls that allow them to avoid the impact of fluctuations in shallow soil water sources, resulting in lower seasonal LFMC variations (Balaguer-Romano *et al.*, 2022). Also, species-specific physiological and anatomical traits drive xylem vulnerability patterns that result in different responses to water stress across co-occurring plant species subjected to the same drought intensity (Choat *et al.*, 2018). Thus, by considering species-specific pressure–volume curves when leaf water potential (Ψ_{leaf}) is at both, below and above the turgor loss point (Ψ_{tlp}), fully mechanistic modeling approaches enabled the modeling of two different response phases of LFMC with respect to plant water status. That is, following seasonal drought, both soil water potential (Ψ_{soil}) and Ψ_{leaf} began to decline leading to a linear reduction in LFMC until the turgor loss point is reached. However, once the Ψ_{tlp} is reached, LFMC declines exponentially as soil dryness increases (Nolan *et al.*, 2020). Thus, the consideration of both linear and nonlinear species-specific relations between LFMC and water status resulted in more accurate LFMC predictions when using fully mechanistic approaches than the semimechanistic approach that only estimates LFMC responses below Ψ_{tlp} by applying a general (logarithmic) relation to all species (Fig. 3; Tables S4, S5). A higher degree of detail when representing mechanistic processes (i.e. $LFMC_{full3}$ vs $LFMC_{full2}$ and $LFMC_{full1}$) also resulted in more accurate LFMC predictions at each species-site combination (Fig. 2b). That is, the modeling of variation in moisture content independently for leaves and stems compartments and the consideration of seasonal changes in their relative proportions following defoliation processes in the $LFMC_{full3}$ mechanistic approach generally improved the simulation of LFMC seasonal dynamics in both the upper and the lower range (exemplified in Fig. 5a). This is consistent with the need of accounting for a potential effect of hydraulic traits segmentation to model LFMC as recently reported (Cakpo *et al.*, 2024). Moreover, the use of hydraulic trait data obtained from field measurements or trait databases instead from model imputations significantly enhanced the accuracy of LFMC predictions obtained through the $LFMC_{full3}$ modeling approach (Fig. 4). Therefore, a promising way to surpass current LFMC prediction capabilities relies on the inclusion of plant physiological processes not always accounted for in process-based models (Torres-Ruiz *et al.*, 2023). It would also be desirable to expand plant trait databases to include missing key traits or species, such as shrub species whose hydraulic traits remain understudied compared to tree species ones. This can be particularly important as shrub species may show significant level of trait intraspecific variation (e.g. López *et al.*, 2021). Importantly, when facing input data limitations such as the lack of accurate soil TAW estimates or reliable data on species-specific hydraulic traits, the use of a semimechanistic modeling approach could result in more accurate and robust LFMC predictions due to the robustness of its empirical nature (Figs 2b, 5b; Table S5). Nonetheless, it also should be considered that the equation used in the semimechanistic approach (Eqn 2) would need to be recalibrated before it could be applied to model other species or areas beyond the western Mediterranean region (Balaguer-Romano *et al.*, 2022).

Overall, the reported performance of the process-based modeling approach $LFMC_{full3}$ ($R^2 = 0.46$, MAE = 17.2%, $n = 6954$) is in line with previous attempts that have applied different approaches to predict LFMC dynamics in other study regions, time periods and vegetation types. Using drought indices, Ruffault *et al.* (2018) obtained performance metrics ($R^2 = 0.3$, MAE = 15%, $n = 8544$) that were limited by the inability to account for species-specific LFMC dynamics. Remote sensing approaches have been widely applied using different products and techniques. Yebra *et al.* (2018) and Tanase *et al.* (2022) respectively applied MODIS ($R^2 = 0.58$, RMSE = 40%, $n = 360$) and Sentinel ($R^2 = 0.55$, MAE = 15%, $n = 2962$) remote sensing products to predict LFMC dynamics. Marino *et al.* (2020) used remote sensed data to develop empirical models that achieve a high performance ($R^2 = 0.73$, MAE = 12%, $n = 143$) inferring the LFMC dynamics of a shrub species (*Cistus* sp.). Cunill-Camprubí *et al.* (2022) combined remote sensing products with random forests algorithms (CCC = 0.56, MAE = 15.2%, $n = 10\,374$), while Quan *et al.* (2017) combined remote sensed data with radiative transfer models ($R^2 = 0.62$, RMSE = 34.57%, $n = 3034$). Also, the extreme gradient boosting algorithm has been applied to build models that estimate LFMC from remote sensed data ($R^2 = 0.56$, RMSE = 27.2%; Wang & Quan, 2023) and from drought indices ($R^2 = 0.56$, RMSE = 14%, $n = 2000$; Liu *et al.*, 2026). Finally, the integration of remote sensed-derived data into process-based modeling frameworks has recently resulted in a promising way to optimize prediction accuracy ($R^2 = 0.56$, MAE = 7.1%, $n = 1364$; Jia *et al.*, 2026).

Although not addressed in this study, there are additional ways to enhance the accuracy of process-based LFMC predictions. First, a main modeling gap relies on including the simulation of species-specific phenological changes in leaf dry mass (Griebel *et al.*, 2023). While the mechanistic modeling of water flows across the atmosphere–soil–plant continuum has been subject to extensive research (Torres-Ruiz *et al.*, 2023), the modeling of plant carbon seasonal fluctuations and their impact on LFMC estimation remains largely unexplored (Jolly *et al.*, 2025). Thus, including the modeling of species-specific seasonal changes in SLA and leaf thickness following maturation processes would allow the simulation of annual fluctuations in the maximum LFMC value at full hydration ($LFMC_{max}$), a key variable for modeling LFMC dynamics (Eqns 3–5) that is rarely assessed in current modeling frameworks (Brown *et al.*, 2022). Also,

improving the mechanistic representation of species-specific drought-related leaf area dynamics, which are yet poorly captured in models, is crucial to enhance the accuracy of process-based modeling predictions (Choat *et al.*, 2018). Thus, although in this study, we focused on mature stage leaves, as it is the most critical in terms of fire danger, the inclusion of processes leading to leaf maturation could improve the estimation of LFMC dynamics. Also, physiological processes affecting canopy leaf area such as drought-related leaf shedding, postdrought shoot flushing or programmed leaf senescence should be included in both process-based modeling frameworks and field measurements (Ruffault *et al.*, 2023; Cakpo *et al.*, 2024). This would lead to considering the ratio of dead-to-live fuels at the canopy level, allowing us to monitor not only LFMC dynamics but also the moisture content of the entire canopy layer (i.e. canopy FMC), enhancing the accuracy of wildfire danger assessments (Balaguer-Romano *et al.*, 2020; Ruffault *et al.*, 2023). However, it should also be considered that the inclusion of new processes in process-based modeling frameworks also entails the potential to increase uncertainty on simulation results as model complexity increases. The availability of observed data at subweekly time scales and regional spatial scales should also be considered as a limiting factor in the process-based modeling of LFMC. A potential shortcut to overcome the use of monitoring networks data relies on the integration of remote sensing products in process-based models through data assimilation approaches (Pasetto *et al.*, 2018; Rojas-Munoz *et al.*, 2023). As these approaches integrate remotely sensed real-time observations, they allow the adjustment of process-based models' initial conditions, reducing uncertainties and potentially enhancing the accuracy of short-term forecasts at large spatial scales (Jia *et al.*, 2026). Ultimately, this will pave the way for developing an operational tool that produces wildfire danger forecasts at subweekly scales to support firefighting resources allocation during a fire season, as well as providing advance warning to local populations.

Acknowledgements

We acknowledge Pere Casals and Ruth Delgado for their participation in the field campaigns of the Catalan LFMC Network database. Also, we acknowledge Kevyn Raynal for his support in the use of the Reseau–Hydrique LFMC database. This publication is part of the 'Severo Ochoa' Centres of Excellence programme, Ref. CEX2023-001340-S, funded by MICIU/AEI/https://doi.org/10.13039/501100011033. Also it was supported by the Spanish Government project IMPROMED (grant no. PID2023-152644NB-I00).

Competing interests

None declared.

Author contributions

RB-R, AS, NM-S, JR, EG, XC, FP and MDC designed the research. NM-S, JR, EG, XC, FP, XL, AD, SD and MDC collected the data. RB-R, AS and MDC performed the research and drafted the manuscript. All authors contributed to the assembly and the completion of the manuscript. RB-R and AS contributed equally to this work.

ORCID

Rodrigo Balaguer-Romano https://orcid.org/0000-0003-2808-6777
Miquel De Cáceres https://orcid.org/0000-0001-7132-2080
Sylvain Delzon https://orcid.org/0000-0003-3442-1711
Arsène Druel https://orcid.org/0000-0002-3938-0085
Xiangzhuo Liu https://orcid.org/0000-0002-1690-7083
Nicolas Martin-StPaul https://orcid.org/0000-0001-7574-0108
François Pimont https://orcid.org/0000-0002-9842-6207
Julien Ruffault https://orcid.org/0000-0003-3647-8172

Data availability

The data and code for analyses and figures are available through GitHub (https://github.com/emf-creaf/LFMC_FR_CAT). Also, the data that support the findings of this study are available in the Supporting Information of this article, specifically in Tables S1–S3.

References

Balaguer-Romano R, De Cáceres M, Espelta JM. 2025. Second-growth forests exhibit higher sensitivity to dry and wet years than long-existing ones. *Ecosystems* **28**: 6.

Balaguer-Romano R, Díaz-Sierra R, De Cáceres M, Cunill-Camprubí À, Nolan RH, Boer MM, Voltas J, Resco de Dios V. 2022. A semi-mechanistic model for predicting daily variations in species-level live fuel moisture content. *Agricultural and Forest Meteorology* **323**: 109022.

Balaguer-Romano R, Díaz-Sierra R, De Cáceres M, Voltas J, Boer MM, Resco De Dios V. 2023. Modeling fuel moisture dynamics under climate change in Spain's forests. *Fire Ecology* **19**: 65.

Balaguer-Romano R, Díaz-Sierra R, Madrigal J, Voltas J, de Dios VR. 2020. Needle senescence affects fire behavior in aleppo pine (*Pinus halepensis* Mill.) stands: a simulation study. *Forests* **11**: 1054.

Bartlett MK, Scoffoni C, Sack L. 2012. The determinants of leaf turgor loss point and prediction of drought tolerance of species and biomes: a global meta-analysis. *Ecology Letters* **15**: 393–405.

Bartlett MK, Sinclair G, Fontanesi G, Knipfer T, Walker MA, McElrone AJ. 2022. Root pressure–volume curve traits capture rootstock drought tolerance. *Annals of Botany* **129**: 389–402.

Boer MM, Resco de Dios V, Stefaniak EZ, Bradstock RA. 2021. A hydroclimatic model for the distribution of fire on earth. *Environmental Research Communications* **3**: 035001.

Brown TP, Hoylman ZH, Conrad E, Holden Z, Jencso K, Jolly WM. 2022. Decoupling between soil moisture and biomass drives seasonal variations in live fuel moisture across co-occurring plant functional types. *Fire Ecology* **18**: 14.

Brown TP, Jolly WM, Conrad ET, Cope Z, Hillman SC. 2025. Combining ecophysiology and combustion traits: a pyro-ecophysiological approach to live fuel moisture prediction in common shrubs. *Fire Ecology* **21**: 53.

Burlett R, Trueba S, Bouteiller XP, Forget G, Torres-Ruiz JM, Martin-StPaul NK, Parise C, Cochard H, Delzon S. 2025. Minimum leaf conductance during drought: unravelling its variability and impact on plant survival. *New Phytologist* **246**: 1001–1014.

Cabon A, Martínez-Vilalta J, Martínez de Aragón J, Poyatos R, De Cáceres M. 2018. Applying the eco-hydrological equilibrium hypothesis to model root distribution in water-limited forests. *Ecohydrology* **11**: e2015.

Cakpo CB, Ruffault J, Dupuy J-L, Pimont F, Doussan C, Moreno M, Jean N, Jean F, Burlett R, Delzon S *et al.* 2024. Exploring the role of plant hydraulics in canopy fuel moisture content: insights from an experimental drought study on *Pinus halepensis* Mill. and *Quercus ilex* L. *Annals of Forest Science* **81**: 26.

Choat B, Brodribb TJ, Brodersen CR, Duursma RA, López R, Medlyn BE. 2018. Triggers of tree mortality under drought. *Nature* **558**: 531–539.

Choat B, Jansen S, Brodribb TJ, Cochard H, Delzon S, Bhaskar R, Bucci SJ, Feild TS, Gleason SM, Hacke UG *et al.* 2012. Global convergence in the vulnerability of forests to drought. *Nature* **491**: 752–755.

Christoffersen BO, Gloor M, Fauset S, Fyllas NM, Galbraith DR, Baker TR, Kruijt B, Rowland L, Fisher RA, Binks OJ *et al.* 2016. Linking hydraulic traits to tropical forest function in a size-structured and trait-driven model (TFS v.1-Hydro). *Geoscientific Model Development* **9**: 4227–4255.

Cunill-Camprubí À, González-Moreno P, Resco De Dios V. 2022. Live fuel moisture content mapping in the Mediterranean basin using Random Forests and combining MODIS spectral and thermal data. *Remote Sensing* **14**: 3162.

Davy R, Kusch E. 2021. Reconciling high resolution climate datasets using KrigR. *Environmental Research Letters* **16**: 124040.

De Cáceres M, Martin-StPaul N, Turco M, Cabon A, Granda V. 2018. Estimating daily meteorological data and downscaling climate models over landscapes. *Environmental Modelling and Software* **108**: 186–196.

De Cáceres M, Mencuccini M, Martin-StPaul N, Limousin JM, Coll L, Poyatos R, Cabon A, Granda V, Forner A, Valladares F *et al.* 2021. Unravelling the effect of species mixing on water use and drought stress in Mediterranean forests: a modelling approach. *Agricultural and Forest Meteorology* **296**: 108233.

De Cáceres M, Molowny-Horas R, Cabon A, Martínez-Vilalta J, Mencuccini M, García-Valdés R, Nadal-Sala D, Sabaté S, Martin-StPaul N, Morin X *et al.* 2023. MEDFATE 2.9.3: a trait-enabled model to simulate Mediterranean forest function and dynamics at regional scales. *Geoscientific Model Development* **16**: 3165–3201.

Druel A, Ruffault J, Davi H, Chanzy A, Marloie O, De Cáceres M, Olioso A, Mouillot F, François C, Soudani K *et al.* 2025. Enhancing environmental models with a new downscaling method for global radiation in complex terrain. *Biogeosciences* **22**: 1–18.

Dukes JS, Xu C, Liao C, Novick KA, Phillips RP, Beverly DP, Fang Y, Jacobs EM, McAdam SAM, Paudel I *et al.* 2026. Improving the representation of plant water stress and water use in Earth System Models. *New Phytologist* **249**: 39–55.

Dumedah G, Walker JP. 2014. Assessment of land surface model uncertainty: a crucial step towards the identification of model weaknesses. *Journal of Hydrology* **519**: 1474–1484.

Duursma RA, Blackman CJ, Lopéz R, Martin-StPaul NK, Cochard H, Medlyn BE. 2019. On the minimum leaf conductance: its role in models of plant water use, and ecological and environmental controls. *New Phytologist* **221**: 693–705.

Fares S, Bajocco S, Salvati L, Camarretta N, Dupuy J-L, Xanthopoulos G, Guijarro M, Madrigal J, Hernando C, Corona P. 2017. Characterizing potential wildland fire fuel in live vegetation in the Mediterranean region. *Annals of Forest Science* **74**: 1.

Gabriel E, Delgado-Dávila R, De Cáceres M, Casals P, Tudela A, Castro X. 2021. Live fuel moisture content time series in Catalonia since 1998. *Annals of Forest Science* **78**: 44.

Griebel A, Boer MM, Blackman C, Choat B, Ellsworth DS, Madden P, Medlyn B, Resco de Dios V, Wujeska-Klause A, Yebra M *et al.* 2023. Specific leaf area and vapour pressure deficit control live fuel moisture content. *Functional Ecology* **719–731**: 37.

Guillemot J, Martin-StPaul NK, Bulascoschi L, Poorter L, Morin X, Pinho BX, le Maire G, RL, Bittencourt P, Oliveira RS *et al.* 2022. Small and slow is safe: on the drought tolerance of tropical tree species. *Global Change Biology* **28**: 2622–2638.

Hoshika Y, Watanabe M, Carrari E, Paoletti E, Koike T. 2018. Ozone-induced stomatal sluggishness changes stomatal parameters of Jarvis-type model in white birch and deciduous oak. *Plant Biology* **20**: 20–28.

Huang L, Bao W, Hu H, Traselin Nkrumah D, Li F. 2023. Rock fragment content alters spatiotemporal patterns of soil water content and temperature: evidence from a field experiment. *Geoderma* **438**: 116613.

Jia Q, Quan X, Resco De Dios V, Yebra M, He B, Li X, Liao Z, Balaguer-Romano R, De Cáceres M. 2026. Enhancing two-week live fuel moisture content forecasts through biophysical modelling and remote sensing data assimilation. *Remote Sensing of Environment* **335**: 115267.

Jolly WM, Conrad ET, Brown TP, Hillman SC. 2025. Combining ecophysiology and combustion traits to predict conifer live fuel moisture content: a pyro-ecophysiological approach. *Fire Ecology* **21**: 19.

Jolly WM, Hadlow AM, Huguet K. 2014. De-coupling seasonal changes in water content and dry matter to predict live conifer foliar moisture content. *International Journal of Wildland Fire* **23**: 480–489.

Jolly WM, Johnson DM. 2018. Pyro-ecophysiology: shifting the paradigm of live wildland fuel research. *Fire* **1**: 1–5.

Kattge J, Bönisch G, Díaz S, Lavorel S, Prentice IC, Leadley P, Tautenhahn S, Werner GDA, Aakala T, Abedi M *et al.* 2020. TRY plant trait database – enhanced coverage and open access. *Global Change Biology* **26**: 119–188.

Larsbo M, Roulier S, Stenemo F, Kasteel R, Jarvis N. 2005. An improved dual-permeability model of water flow and solute transport in the Vadose zone. *Vadose Zone Journal* **4**: 398–406.

Liu X, Martin-StPaul N, Ruffault J, Lai G, Raynal K, Raquel R, Wang H, Parsons R, Dupuy J-L, Pimont F. 2026. Drought indices predict changes in live fuel moisture content (LFMC) across French Mediterranean shrublands: a multisource and machine learning approach. *Agricultural and Forest Meteorology* **381**: 111093.

Loiseau B, Carrière SD, Jougnot D, Singha K, Mary B, Delpierre N, Guérin R, Martin-StPaul NK. 2023. The geophysical toolbox applied to forest ecosystems – a review. *Science of the Total Environment* **899**: 165503.

López R, Cano FJ, Martin-StPaul NK, Cochard H, Choat B. 2021. Coordination of stem and leaf traits define different strategies to regulate water loss and tolerance ranges to aridity. *New Phytologist* **230**: 497–509.

Marino E, Yebra M, Guill M, Algeet N, Tom L, Madrigal J, Guijarro M, Hernando C. 2020. Investigating live fuel moisture content estimation in fire-prone shrubland from remote sensing using empirical modelling and RTM simulations. *Remote Sensing* **12**: 2251.

Martin-StPaul N, Delzon S, Cochard H. 2017. Plant resistance to drought depends on timely stomatal closure. *Ecology Letters* **20**: 1437–1447.

Martin-StPaul N, Pimont F, Dupuy JL, Rigolot E, Ruffault J, Fargeon H, Cabane E, Duché Y, Savazzi R, Toutchkov M. 2018. Live fuel moisture content (LFMC) time series for multiple sites and species in the French Mediterranean area since 1996. *Annals of Forest Science* **75**: 57.

Matthews S. 2014. Dead fuel moisture research: 1991–2012. *International Journal of Wildland Fire* **23**: 78–92.

McNeice W, Griebel A, Krix DW, Murray BR, Boer MM, Choat B, Nolan RH. 2026. Moisture content ranges in live Eucalyptus leaves vary among species and strongly affect ignitability. *Fire Ecology* **22**: 11.

Mencuccini M, Rosas T, Rowland L, Choat B, Cornelissen H, Jansen S, Kramer K, Lapenis A, Manzoni S, Niinemets Ü *et al.* 2019. Leaf economics and plant hydraulics drive leaf: wood area ratios. *New Phytologist* **224**: 1544–1556.

Moreno M, Simioni G, Cochard H, Doussan C, Guillemot J, Decarsin R, Fernandez-Conradi P, Dupuy J-L, Trueba S, Pimont F *et al.* 2024. Isohydricity and hydraulic isolation explain reduced hydraulic failure risk in an experimental tree species mixture. *Plant Physiology* **195**: 2668–2682.

Morris H, Plavcová L, Cvecko P, Fichtler E, Gillingham MAF, Martínez-Cabrera HI, McGlinn DJ, Wheeler E, Zheng J, Ziemińska K *et al.* 2016. A global analysis of parenchyma tissue fractions in secondary xylem of seed plants. *New Phytologist* **209**: 1553–1565.

Muñoz-Sabater J, Dutra E, Agustí-Panareda A, Albergel C, Arduini G, Balsamo G, Boussetta S, Choulga M, Harrigan S, Hersbach H *et al.* 2021. ERA5-Land: a state-of-the-art global reanalysis dataset for land applications. *Earth System Science Data* **13**: 4349–4383.

Myneni R, Knyazikhin Y, Park T. 2021. MODIS/Terra Leaf Area Index/FPAR 8-Day L4 Global 500m SIN Grid V061. ASA EOSDIS Land Processes Distributed Active Archive Center.

Nolan RH, Blackman CJ, Dios RD, Choat B, Medlyn BE, Li X, Bradstock RA, Boer MM. 2020. Linking forest flammability and plant vulnerability to drought. *Forests* **11**: 779.

Nolan RH, Hedo J, Arteaga C, Sugai T, Resco de Dios V. 2018. Physiological drought responses improve predictions of live fuel moisture dynamics in a Mediterranean forest. *Agricultural and Forest Meteorology* **263**: 417–427.

Pasetto D, Arenas-Castro S, Bustamante J, Casagrandi R, Chrysoulakis N, Cord AF, Dittrich A, Domingo-Marimon C, El Serafy G, Karnieli A *et al.* 2018. Integration of satellite remote sensing data in ecosystem modelling at local scales: practices and trends. *Methods in Ecology and Evolution* **9**: 1810–1821.

Pimont F, Ruffault J, Martin-StPaul NK, Dupuy JL. 2019. Why is the effect of live fuel moisture content on fire rate of spread underestimated in field experiments in shrublands? *International Journal of Wildland Fire* **28**: 127–137.

Poggio L, De Sousa LM, Batjes NH, Heuvelink GBM, Kempen B, Ribeiro E, Rossiter D. 2021. SoilGrids 2.0: producing soil information for the globe with quantified spatial uncertainty. *The Soil* **7**: 217–240.

Quan X, Chen R, Yebra M, Riaño D, Resco de Dios V, Li X, He B, Nolan RH, Griebel A, Boer MM *et al.* 2024. Sub-daily live fuel moisture content estimation from Himawari-8 data. *Remote Sensing of Environment* **308**: 114170.

Quan X, He B, Yebra M, Yin C, Liao Z, Li X. 2017. Retrieval of forest fuel moisture content using a coupled radiative transfer model. *Environmental Modelling & Software* **95**: 290–302.

Resco De Dios V. 2020. *Plant-fire interactions: applying ecophysiology to wildfire management*. Cham: Springer International Publishing.

Resco de Dios V, Fellows AW, Nolan RH, Boer MM, Bradstock RA, Domingo F, Goulden ML. 2015. A semi-mechanistic model for predicting the moisture content of fine litter. *Agricultural and Forest Meteorology* **203**: 64–73.

Robbins Z, Guthrie W, Killebrew A, Salinas L, Matheny AM, Cabraal S, Ulatowski M, Trader L, Atchley A, Linn R *et al.* 2025. Ponderosa pine hydraulic stress predicts more extreme wildfire behavior under future conditions in Bandelier National Monument. *NM. Fire Ecology* **21**: 64.

Rodrigues M, Cunill Camprubí À, Balaguer-Romano R, Coco Megía CJ, Castañares F, Ruffault J, Fernandes PM, Resco de Dios V. 2023. Drivers and implications of the extreme 2022 wildfire season in Southwest Europe. *Science of the Total Environment* **859**: 160320.

Rojas-Munoz O, Calvet J-C, Bonan B, Baghdadi N, Meurey C, Napoly A, Wigneron J-P, Zribi M. 2023. Soil moisture monitoring at kilometer scale: assimilation of Sentinel-1 products in ISBA. *Remote Sensing* **15**: 4329.

Ruffault J, Limousin J, Pimont F, Dupuy J, De Càceres M, Cochard H, Mouillot F, Blackman CJ, Torres-Ruiz JM, Parsons RA *et al.* 2023. Plant hydraulic modelling of leaf and canopy fuel moisture content reveals increasing vulnerability of a Mediterranean forest to wildfires under extreme drought. *New Phytologist* **237**: 1256–1269.

Ruffault J, Martin-StPaul N, Pimont F, Dupuy JL. 2018. How well do meteorological drought indices predict live fuel moisture content (LFMC)? An assessment for wildfire research and operations in Mediterranean ecosystems. *Agricultural and Forest Meteorology* **262**: 391–401.

Ruffault J, Pimont F, Cochard H, Dupuy JL, Martin-Stpaul N. 2022. SurEau-Ecos v2.0: a trait-based plant hydraulics model for simulations of plant water status and drought-induced mortality at the ecosystem level. *Geoscientific Model Development* **15**: 5593–5626.

Sanchez-Martinez P, Martínez-Vilalta J, Dexter KG, Segovia RA, Mencuccini M. 2020. Adaptation and coordinated evolution of plant hydraulic traits. *Ecology Letters* **23**: 1599–1610.

Sánchez-Pinillos M, De Cáceres M, Casals P, Alvarez A, Beltrán M, Pausas JG, Vayreda J, Coll L. 2021. Spatial and temporal variations of overstory and understory fuels in Mediterranean landscapes. *Forest Ecology and Management* **490**: 119094.

Saponaro V, De Cáceres M, Dalmonech D, D'Andrea E, Vangi E, Collalti A. 2025. Assessing the combined effects of forest management and climate change on carbon and water fluxes in European beech forests. *Forest Ecosystems* **12**: 100290.

Shangguan W, Hengl T, Mendes De Jesus J, Yuan H, Dai Y. 2017. Mapping the global depth to bedrock for land surface modeling. *Journal of Advances in Modeling Earth Systems* **9**: 65–88.

Sitch S, Smith B, Prentice IC, Arneth A, Bondeau A, Cramer W, Kaplan JO, Levis S, Lucht W, Sykes MT *et al.* 2003. Evaluation of ecosystem dynamics, plant geography and terrestrial carbon cycling in the LPJ dynamic global vegetation model. *Global Change Biology* **9**: 161–185.

Stocker BD, Tumber-Dávila SJ, Konings AG, Anderson MC, Hain C, Jackson RB. 2023. Global patterns of water storage in the rooting zones of vegetation. *Nature Geoscience* **16**: 250–256.

Tanase MA, Nova JPG, Marino E, Aponte C, Tomé JL, Yáñez L, Madrigal J, Guijarro M, Hernando C. 2022. Characterizing live fuel moisture content from active and passive sensors in a Mediterranean environment. *Forests* **13**: 1846.

Tavşanoğlu Ç, Pausas JG. 2018. A functional trait database for Mediterranean Basin plants. *Scientific Data* **5**: 180135.

Thornton PE, Shrestha R, Thornton M, Kao S-C, Wei Y, Wilson BE. 2021. Gridded daily weather data for North America with comprehensive uncertainty quantification. *Scientific Data* **8**: 190.

Torres-Ruiz JM, Cochard H, Delzon S, Boivin T, Burlett R, Cailleret M, Corso D, Delmas CEL, De Caceres M, Diaz-Espejo A *et al.* 2023. Plant hydraulics at the heart of plant, crops and ecosystem functions in the face of climate change. *New Phytologist* **241**: 984–999.

Walker AP, Beckerman AP, Gu L, Kattge J, Cernusak LA, Domingues TF, Scales JC, Wohlfahrt G, Wullschleger SD, Woodward FI. 2014. The relationship of leaf photosynthetic traits – V_{cmax} and J_{max} – to leaf nitrogen, leaf phosphorus, and specific leaf area: a meta-analysis and modeling study. *Ecology and Evolution* **4**: 3218–3235.

Wang L, Quan X, He B, Yebra M, Xing M, Liu X. 2019. Assessment of the dual polarimetric Sentinel-1a data for forest fuel moisture content estimation. *Remote Sensing* **11**: 1568.

Wang W, Quan X. 2023. Estimation of live fuel moisture content from multiple sources of remotely sensed data. *IEEE Geoscience and Remote Sensing Letters* **20**: 1–5.

Yebra M, Quan X, Riaño D, Rozas Larraondo P, Van Dijk AIJM, Cary GJ. 2018. Mapping live fuel moisture content and flammability for continental Australia using optical remote sensing. International Geoscience and Remote Sensing Symposium (IGARSS), 5903–5906.

Yebra M, Scortechini G, Adeline K, Aktepe N, Almoustafa T, Bar-Massada A, Beget ME, Boer M, Bradstock R, Brown T *et al.* 2024. Globe-LFMC 2.0, an enhanced and updated dataset for live fuel moisture content research. *Scientific Data* **11**: 332.

Supporting Information

Additional Supporting Information may be found online in the Supporting Information section at the end of the article.

Fig. S1 MAE distribution across TAW values.

Fig. S2 Plant traits precedence and modeling approaches performance.

Fig. S3 Time series and fit of observed and predicted LFMC for each species-site combination.

Note S1 Decomposition of maximum fuel moisture content (FMCmax) into leaf (MCleaf) and stem (MCstem) components.

Table S1 Summary of study sites.

Table S2 Summary of observed LFMC data.

Table S3 Species-specific anatomical and physiological parameters.

Table S4 Best simulations fit for each species-site combination.

Table S5 Simulation performance for each species.

Please note: Wiley is not responsible for the content or functionality of any Supporting Information supplied by the authors. Any queries (other than missing material) should be directed to the *New Phytologist* Central Office.

Disclaimer: The New Phytologist Foundation remains neutral with regard to jurisdictional claims in maps and in any institutional affiliations.